Medical Physics
The International Journal of Medical Physics Research and Practice

The indirect use of CT numbers to establish material properties needed for Monte Carlo calculation of dose distributions in patients

F. C. P. du Plessis, C. A. Willemse, M. G. Lötter, and L. Goedhals

Citation: Medical Physics **25**, 1195 (1998); doi: 10.1118/1.598297
View online: http://dx.doi.org/10.1118/1.598297
View Table of Contents: http://scitation.aip.org/content/aapm/journal/medphys/25/7?ver=pdfcov
Published by the American Association of Physicists in Medicine

The indirect use of CT numbers to establish material properties needed for Monte Carlo calculation of dose distributions in patients

F. C. P. du Plessis,[a] C. A. Willemse, and M. G. Lötter
Biophysics Department, Faculty of Medicine, University of the Free State, P.O. Box 339, Bloemfontein, 9300 South Africa

L. Goedhals
Department of Radiation Oncology, National Hospital, Roth Avenue, Bloemfontein, 9301 South Africa

(Received 25 June 1997; accepted for publication 30 April 1998)

A number of Monte Carlo codes are available, which can be used to calculate dose distributions in patients with high accuracy. Patient geometry can readily be derived with adequate spatial resolution from CT scans. To perform the Monte Carlo calculation with the same spatial resolution, it is necessary to enter the atomic composition and density of the tissue in each voxel of the CT image. This means entering 65 536 discrete values for a CT slice with a 256×256 matrix size. The need for automated methods of setting up the material data files is obvious. Because there is no direct unique relationship between CT numbers and material composition, the aim of our work was to devise a method whereby the atomic composition and density in each voxel could be assigned automatically by indirect derivation from the CT numbers. The set of all tissues types in the human body was divided into subsets that are dosimetrically equivalent, based on Monte Carlo calculated depth dose curves in homogeneous phantoms of each tissue. CT number ranges corresponding to each tissue subset were determined from the calibration curve linking electron density with CT number for the specific CT scanner. Further subdivision was found to be necessary for the lung and bone type tissues. This was done by keeping the atomic composition constant and varying the physical density. It was found that 57 distinct tissue subsets were needed to represent the 16 main tissue types in the body at a 1% dose level. Corresponding CT number intervals of 30 HU were needed in the lung and soft tissue region, whereas in the bone region the intervals could be increased to 100 HU. A computer algorithm was set up to convert automatically from CT number to corresponding equivalent material number for the Monte Carlo preprocessor code. [S0094-2405(98)01507-7]

Key words: Monte Carlo, CT number, tissue composition, patient dose distributions

I. INTRODUCTION

A number of Monte Carlo codes are available, for example, EGS4,[1] ITS3,[2] MCNP,[3] and PEREGRINE[4] which can be used to calculate dose distributions in patients with high accuracy. The degree of accuracy that can be attained is determined mainly by the following factors: (a) The accuracy of the cross section data used for simulating the various interactions between ionizing radiation and matter; (b) How accurately the radiation beams are modeled with respect to energy and directional distribution; (c) The statistical accuracy of the Monte Carlo calculation method, which is mainly determined by the number of histories followed; and d) How accurately the patient geometry and tissue properties relevant to the radiation interactions are modeled.

The accuracy of the cross section data has been discussed by Rogers and Bielajew.[5] The characteristics of the radiation beams of a particular accelerator can also be determined by Monte Carlo simulation, e.g., using the EGS4 based Code BEAM.[6] The accuracy obtainable with this code has been discussed by Rogers *et al.*[6] The statistical accuracy can be improved by following enough histories. This is, however, limited by the speed of the computers available and therefore the method cannot be used for routine treatment planning of patients yet. It is envisaged that with the continued development of computing technology this may be feasible in future. This paper addresses the fourth issue namely the accurate representation of patient properties in a Monte Carlo program. The patient geometry can readily be derived with adequate spatial resolution from CT scans of the patient. A common image matrix size of 256×256 pixels will lead to pixel sizes of the order of 2 mm for most patients.

To specify the material properties of the tissue to be used in the MC algorithm, it is necessary to enter the atomic composition and density of the tissue in each voxel.[1] This means entering 65 536 discrete values per CT slice. The need for automated methods of setting up the necessary data files is obvious. One approach to reduce the number of data values, is the method of Manfredotti *et al.*,[7] who reduced the number of voxels by a union algorithm. In their method the user selects some intervals of CT numbers and assigns a material to each interval. The relationship between CT number and material used in this method is not described. Because there is no direct unique relationship between CT numbers and material composition, the aim of our work was to devise a method whereby the atomic composition and density of each

voxel could be specified automatically by indirect derivation from the CT numbers.

In our work, we use a modified definition of CT numbers, as employed by our treatment planning system, namely:

$$H = 1000\left(1 + \frac{\mu - \mu_w}{\mu_w}\right),$$

where μ and μ_w are the linear attenuation coefficients of the medium and water, respectively. This amounts to an offset of scale where water has a CT number of 1000 HU, rather than the conventional value of zero. Our method is based on the following assumptions: (1) the Hounsfield numbers for a given CT scanner's effective energy will be uniquely determined by the atomic composition and physical density of the tissue in each voxel (ignoring image artifacts); and (2) the dose due to a given megavoltage radiation beam at any point within a homogeneous tissue will also be uniquely determined by the tissue's atomic composition and physical density.

For a given level of accuracy desired in the Monte Carlo dose computation (say 1%), and given enough histories to make the statistical variation negligible, it is possible to divide the set of all tissue types into subsets, where the tissues in each subset are dosimetrically equivalent. The tissues falling in any particular subset can then be represented by any member of the subset. Once the dosimetrically equivalent tissue subsets have been determined, corresponding CT number intervals can be determined from the calibration curve linking electron density to Hounsfield values for the CT scanner.

II. METHODS

A. Determination of dosimetrically equivalent tissue subsets

In order to classify the different tissues in the human body according to dosimetric equivalence in a megavoltage photon beam, a Monte Carlo simulation was done using the CYLTRAN option of the ITS3[2] code.

Homogeneous, cylindrical phantoms with outer diameters of 20 cm and length 20 cm were modeled. A pencil beam of 8 MV photons was directed parallel to the cylinder axis and was incident perpendicularly at the center of the circular end surface. The photon energy was sampled from a cumulative function derived from a previous Monte Carlo simulation of the radiation head of a Philips SL75/14 linear accelerator. Energy deposition kernels for one million histories were scored in radial annuli of 2 mm width between 0 and 4 cm radius, and 1 cm width beyond 4 cm radius. The depth dimension was divided into zones which had a thickness of 2 mm from 0 to 4 cm depth and a 1 cm thickness beyond 4 cm depth. Doses along the central axis for a 100 cm^2 circular field size (simulating a 10 cm$\times$10 cm field) were subsequently calculated using these kernels. The statistical variation in the dose along the central axis was less than one percent in all scoring zones.

Monte Carlo simulations were performed for the 16 most common tissue types (including water) found in the human body, as given in ICRU report 44[8] (see Table I). The average densities given in the report were used for each tissue. The depth dose curves obtained from these simulations were compared with that of water. A percentage depth dose was calculated by normalizing the dose values for each of the different tissue types to the global maximum dose found for all the tissues. The percentage depth dose curve of each tissue type was subtracted from that of water and these percentage differences as a function of depth (phantom thickness) were smoothed by fitting a quadratic polynomial to each of the curves beyond a depth of 2 cm to a depth of 20 cm. The correlation was better than 0.99 for each fit. This procedure was adopted to reduce the effect of the one percent statistical noise level of the Monte Carlo simulations. This allowed a separation between the various tissue types at the one percent dose level.

TABLE I. The different tissue types and the subsets into which they are separated based on the percentage difference in depth dose obtained with CYLTRAN based Monte Carlo simulations. Electron density values for the different tissue types were taken from ICRU 44. The two columns on the right shows the CT number ranges associated with each subset of materials.

Subset	Tissue	Electron density ($m^{-3}\times10^{26}$)	Lower CT# limit	Upper CT# limit
1	Lung (inflated)	862	20	950
2	Adipose	3180	951	980
3	Water	3340	981	1010
4	Brain	3460	1011	1040
	Breast	3390		
	Pancreas	3460		
	Redmarrow	3420		
5	Heart	3510	1041	1070
	Kidney	3480		
	Thyroid	3480		
	Lung(deflated)	3480		
	Liver	3510		
	Muscle	3480		
	Spleen	3510		
6	Cartilage	3520	1071	1100
7	Cortical bone	5950	1101	3000

B. Derivation of CT number intervals

The electron densities of all the tissues used in this study are also reported in ICRU 44.[8] Using these values, the range of electron densities in each tissue subset was determined. The corresponding range of CT numbers for each subset was found from a calibration curve, which was obtained by scanning a RMI CT density phantom (Gammex RMI, Middleton, WI) in a Siemens Somatom HiQ-S CT scanner. The CT density phantom contains inserts of different tissue equivalent materials spanning the range of electron densities from adipose tissue to cortical bone. The effect of different atomic numbers is therefore also inherently included in the calibration curve. A one-to-one relationship was thus established between CT number intervals and tissue subsets. To investi-

gate the influence of variation in physical density of lung and bone on the depth dose curve, Monte Carlo simulations as described in the previous section were also done for these two tissue types for a range of different physical densities. In this way, the lung and bone tissues were subdivided into tissue subsets with the same atomic composition, but different physical densities.

The depth dose data for the soft tissues (subsets 2–5 in Table I) were analyzed at four different depths, namely 5, 10, 15, and 20 cm. At each depth, the percentage dose value of each tissue type, calculated as described in Sec. A, was subtracted from the percentage dose value of adipose, the latter being the tissue with the lowest CT number in this combined group of tissues. The percentage difference was plotted against CT number. The CT numbers were calculated by using a CT calibration curve linking each tissue's relative electron density to a unique CT number.

C. Conversion of CT numbers to material types

Monte Carlo codes such as CYLTRAN and EGS4 use preprocessor programs to calculate the relevant cross section data for the materials and energy span used in the particle transport simulations. These programs need as input the atomic composition and physical density of each material. The input data files require a discrete set of material specifications. Each tissue subset defined above was thus set up as a material type represented by a number in the input data file of the preprocessor. The atomic composition and density of one member of a subset, as found in ICRU 44, was used as representative of the subset. A FORTRAN program was written to read CT images and to convert each pixel's CT number into the corresponding material number.

III. RESULTS

A. Dosimetrically equivalent tissue subsets

In Fig. 1 the percentage difference with respect to water of the depth dose curves of all the tissues excluding adipose, cortical bone, cartilage and inflated lung are shown. Figure 2 shows the corresponding curves for various densities of lung and adipose tissue and Fig. 3 for various densities of cortical bone and cartilage.

These data were used to separate the tissues into subsets, such that the members in each subset differed by less than one percent in depth dose. The resulting tissue subsets are shown in Table I.

B. CT number intervals

Figure 4 shows the percentage difference in dose between each of the soft tissues and adipose tissue, against CT number, at depths of 5, 10, 15, and 20 cm. The same procedure was repeated for various densities of inflated lung and cortical bone as can be seen in Figs. 5 and 6. The change of normalization material from water to adipose tissue is done to enable an expanded ordinate scale to be used in Figs. 4, 5, and 6 for clarity.

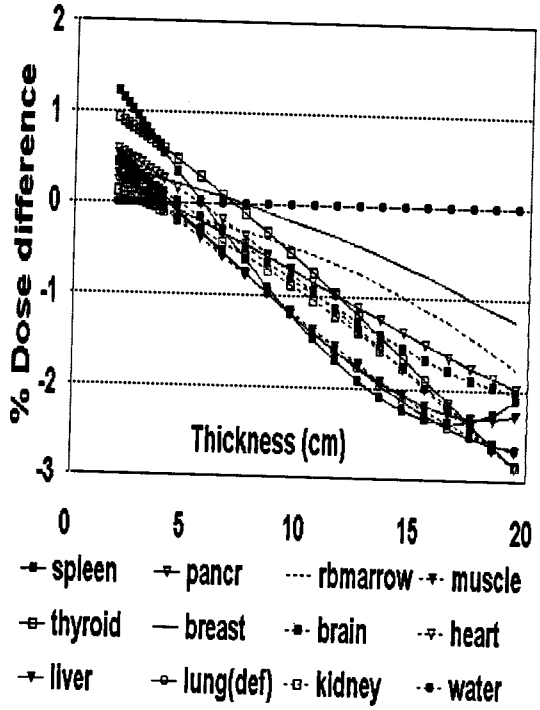

FIG. 1. The percentage difference in depth dose relative to water of various tissue types obtained from depth dose simulations with Monte Carlo methods. These data were obtained after the original depth dose data were smoothed with quadratic functions over the range 2 cm to 20 cm and each tissue type's smoothed percentage depth dose curve was subtracted from that of water.

From each of these graphs the CT number interval corresponding to a dose variation not exceeding one percent, was determined. This was calculated from the inverse of the slope of the graphs in Figs. 4–6, which represents the change in CT number per unit percentage dose difference. Figure 7

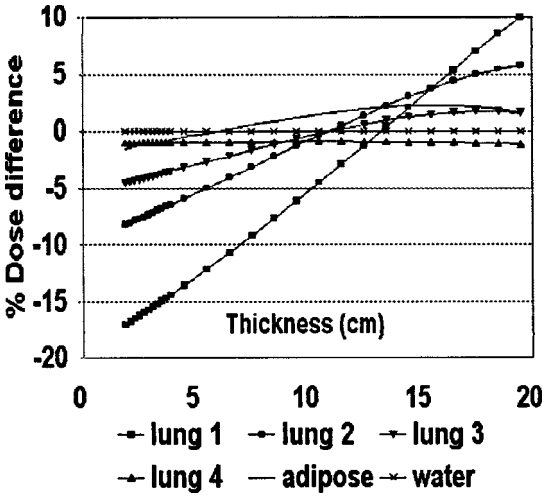

FIG. 2. The percentage difference in depth dose relative to water of various densities (in g/cm^3) of lung (lung1=0.6, lung2=0.8, lung3=0.9, lung4 =1.0) and adipose tissue obtained from depth dose simulations with Monte Carlo methods. These data were obtained after the original depth dose data were smoothed with quadratic functions over the range 2 cm to 20 cm and each tissue type's smoothed percentage depth dose curve was subtracted from that of water.

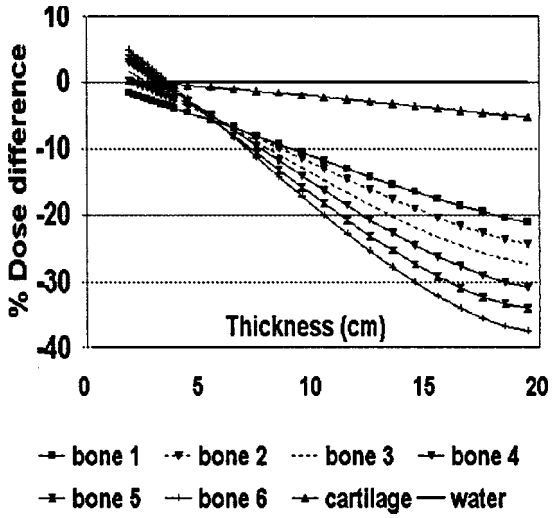

FIG. 3. The percentage difference in depth dose relative to water of various densities (in g/cm^3) of skeletal bone (bone1=1.4, bone2=1.6, bone3=1.8, bone4=1.9, bone5=2.0, bone6=2.2) and cartilage obtained from depth dose simulations with Monte Carlo methods. These data were obtained after the original depth dose data were smoothed with quadratic functions over the range 2 cm to 20 cm and each tissue type's smoothed percentage depth dose curve was subtracted from that of water.

shows these inverse slopes as a function of tissue thickness. For cartilage, soft tissue and lung, a CT number interval of about 30 HU, and for cortical bone a CT number interval of about 100 HU would result in dose differences of less than one percent.

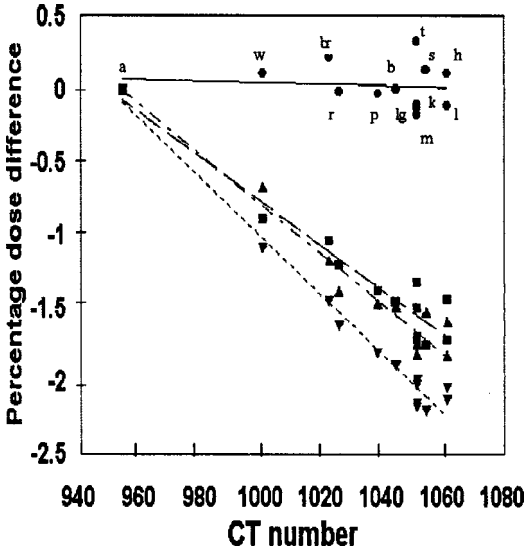

FIG. 4. The percentage dose difference obtained by subtracting the depth dose data of various soft tissues from the dose of adipose tissue at depths of 5 (—), 10 (– — –), 15 (···) and 20 (––) cm. The lines are the linear fitted data and the markers represent the 12 different soft tissue types, each labeled in dataset 2 (depth 10 cm) according to a = adipose, w = water, br = breast, r = redmarrow, p = pancreas, t = thyroid, s = spleen, h = heart, l = liver, lg = lung(deflated), b = brain, k = kidney, m = muscle.

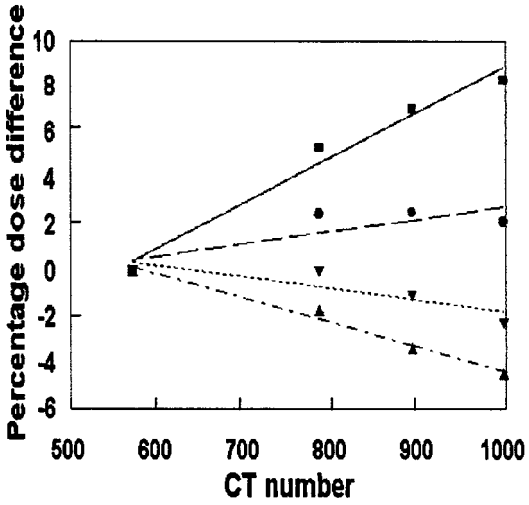

FIG. 5. The percentage dose difference for lung phantoms of different density at depths of 5 (—), 10 (– — –), 15 (···) and 20 (– –) cm. This was obtained in the same manner as in Fig. 4 but subtraction was done from the dose of the lung having the lowest density (CT number = 570).

C. Conversion of CT numbers to material types

Figure 7 indicates that the maximum allowable CT number interval can be taken as 30 HU for inflated lung and all the soft tissues up to subset 6 in Table I. For the bone type tissues (subset 7 in Table I) the maximum CT number interval was chosen as 100 HU. These CT number intervals will minimize the effect of phantom (organ) thickness. A FORTRAN program was written to read CT images and to convert each pixel's CT number into a corresponding material number. A flowchart of the program is shown in Fig. 8. The procedure consists of setting up a series of bins between the CT numbers 0 and 1100 with equal width of 30 HU and to repeat it over the range of 1100 to 3000 with equal widths

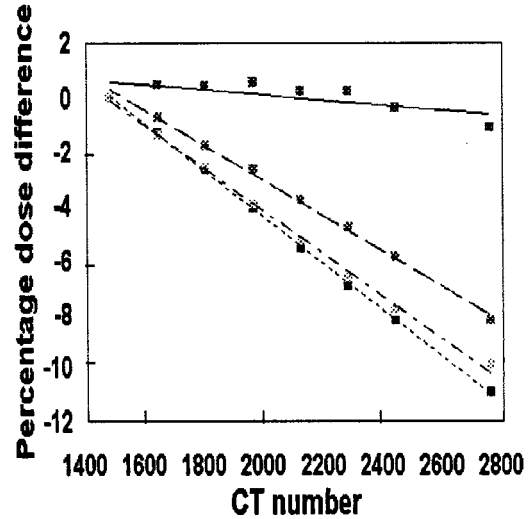

FIG. 6. The percentage dose difference as in Figs. 4 and 5 for different densities of hard bone.

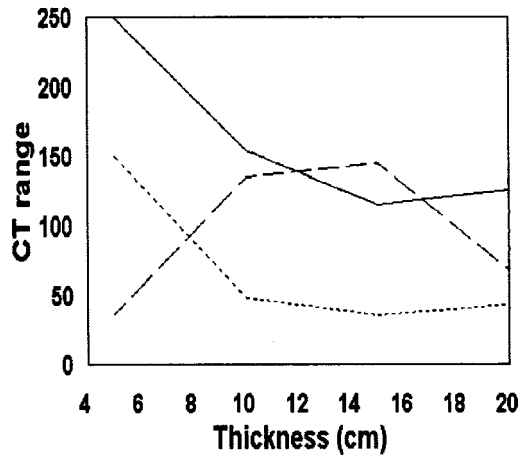

FIG. 7. The CT number intervals calculated from the slopes of the graphs in Figs. 4–6, for cortical bone (—), soft tissue (- - -) and lung (···).

of 100 HU. A CT image's pixels are read and the bins in which these pixels will fall are determined. Each pixel value is then set to the bin number, which in turn is linked to a material type.

These materials are chosen from any of those found in the 7 subsets of materials listed in Table I with the restriction that precisely one can be chosen out of each subset. As can be seen from Table I, each one of subsets 2 to 6 spans a CT number range of 30 HU, exactly one bin width. However subsets 1 and 7 each spans a range of CT numbers containing several bin widths, i.e., 32 for lung and 19 for bone. In order to assign a material type to each of these bins the basic composition of lung and bone is used but their physical densities are varied in steps, leading, via the corresponding electron densities, to CT numbers covering the desired range. This correlates with the fact that lung and bone densities of a patient population are variable, and not fixed as in Table II.

In our application we have chosen one material out of each subset as shown in Table II. Note that any of the other materials in the subsets would also suffice, provided that only one material from each of the 7 subsets is chosen. These materials serve as the basis for constructing an input file for Monte Carlo programs since each of these programs have a preprocessor program which calculates each material's cross section data. They all need the atomic components, weight fractions and physical density of each material in order to do these calculations (see Table II).

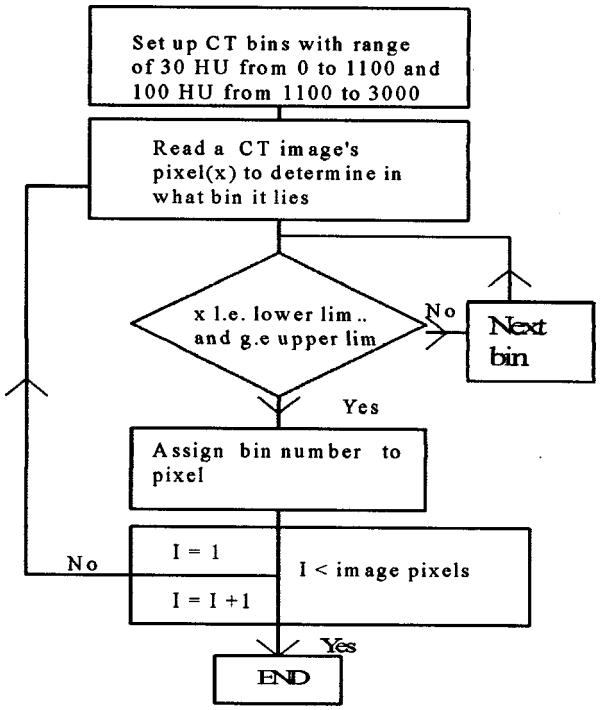

FIG. 8. The basic operation of converting a CT image into one suitable for use with Monte Carlo simulations. As a first step the program calculates a series of bin intervals ranging from CT number 0 to 1100 with equal width of 30 HU, and bin intervals of 100 HU for CT numbers between 1100 and 3000. A CT image's pixels are read and it is determined in which CT intervals (bins) they will fall by determining the upper limit and the lower limit of the particular intervals. The pixel value is then converted to the bin number, which in turn is linked to a certain material type.

IV. DISCUSSION

The percentage dose versus phantom thickness shown in Fig. 1 can be interpreted as follows: Consider a cros sectional transverse slice of a patient with a homogeneous organ marked (shaded area) as shown in Fig. 9. An 8 MV photon beam is directed from the left and travels a distance *d* before reaching the organ. If the organ belongs to a subset in Table I in which there are two or more members, then any member of the subset can be used to identify the tissue type of the organ. The dose difference between the different types of tissue will be within one percent if the organ's dimensions do not exceed 20 cm in the direction of the beam, which in this study is assumed to be the maximum organ thickness.

Thus the data shown in Fig. 1 should be interpreted as organ thickness data (rather than depth dose data in the conventional sense) in which the cumulative effect on the dose is shown for the same incident photon fluence.

This percentage dose data is shown in Table I, with the criterion that in each subset its members are dosimetrically equivalent at the one percent level. Note that water falls into a subset of its own, indicating that it differs significantly from other soft tissue types when comparing dosimetric character. This is mainly because its electron density differs to such an extent from other tissue types that the dose scored in water will deviate significantly from soft tissue as its thickness increases. This in effect dismisses the general idea that all soft tissue types can be treated as strictly water equivalent when interested in dose differences at the one percent level. On a global scale all of the soft tissues, including water, will be dosimetrically the same if discrimination is done at the 3 to 5 percent level. The main factor which influences the dose in tissues is the electron density, which governs the Compton interaction process. For a typical 8 MV photon spectrum this contributes as much as 98% of all the interactions in the phantoms, with the remainder consisting mainly of pair production. The effect of pair production on the dose can be observed from Fig. 4 as a spread in percent-

TABLE II. The chosen materials with their atomic compositions shown as percentage weight fractions and physical density (ρ), for use in a Monte Carlo preprocessing program which calculates cross section data. This was assembled by taking one material type from each subset in Table I and using its atomic composition data and average density as found in ICRU 44. Note that the densities given for lung and bone are average values and that the variable densities of these tissues were taken into account by introducing additional material subsets.

Tissue	H	C	N	O	Na	S	Cl	P	K	Fe	Ca	ρ (g/cm^3)
Lung	10.3	11.0	3.1	74.9	0.2	0.3	0.3	0.2	0.2			0.28
Adipose	11.4	60.0	0.7	27.8	0.1	0.1	0.1					0.95
Water	11.2			88.8								1.00
Brain	10.7	15.0	2.2	71.2	0.2	0.2	0.3	0.4	0.3			1.04
Heart	10.3	12.0	3.2	73.4	0.1	0.2	0.3	0.1	0.2	0.1		1.06
Cartilage	9.6	10.0	2.2	74.4	0.5	0.9	0.3	2.2				1.10
Cortical bone	3.4	16.0	4.2	43.5	0.1	0.3		10.3			22.5	1.92

age dose values around the regression line of different soft tissue types having the same CT number. This deviation of the percentage dose is in the order of 0.25 percent, suggesting that the pair production component has a small influence in this photon energy range. This can be readily observed when comparing the percentage dose of tissue types having the same CT number like thyroid, kidney and muscle at around 1050 HU.

The method of assigning a tissue type to a CT pixel of a patient's CT slice data has some implications. If a patient's organs have densities lying outside the limits of the subsets set up in the preprocessor input file then it would be assigned to a tissue in another subset of soft tissue. However, due to the fact that the Compton scatter process dominates the photon interactions this means that the dose scored in that organ will still be accurate enough since its atomic composition (which influences the pair production process) does not lead to a large change in dose. This is seen in Fig. 4 where tissues having the same CT number only differ in dose by a total of 0.5% in the worst case. The factor of prime importance is the electronic density of the material. We decided against the idea of assigning each of the material types to water and modulating its electron density to match those of the subset members mainly because the effect of this on the pair production process was not studied. We make the assumption that the dose difference between materials would not be altered too much if it is assigned to a member of a particular subset in which the pair production effect is already inherently accounted for.

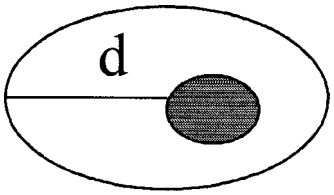

FIG. 9. A model of a CT slice of a patient. Radiation is incident from the left and travels a distance d before reaching the homogeneous shaded organ. The choice of material for the organ does not change the dose in the organ by more than one percent provided that the choice was made out of members of the same subset (see Table I).

Figure 7 shows the behavior of the maximum bin width in Hounsfield units as a function of organ thickness. For cortical bone it reaches a minimum of around 115 HU at a thickness of 15 cm, indicating that the dose variation in bone, as a function of HU, would be a maximum at this thickness. For soft tissues the minimum bin width is 35 HU. Deflated lung tissue have nearly the opposite effect compared to soft tissue. The main reason is that the less dense it becomes (more inflated with air) the deeper the dose maximum occurs, creating a larger sensitivity of percentage dose on density than deeper in the lung at a thickness larger than 15 cm. From this analysis the maximum bin width for lung tissue was determined as 34 HU, equaling that of other soft tissue types. In our study it was decided to use a soft tissue bin width of 30 HU and for cortical bone 100 HU. This conclusion is strictly valid only for the beam energy used namely 8 MV. Consideration of the physical principles indicates that for lower energy beams the 1% bin widths will have to be decreased. This implies that for different energy beams an optimized bin structure must be found according to the methods described here.

The input data file for a Monte Carlo preprocessor program was constructed from 7 basic tissue types and by modulating the physical density for deflated lung tissue and cortical bone, 57 different tissue types (excluding air) could be constructed, spanning a total CT range of 3000 HU. The division was: 21 types of cortical bone ranging from 1100 to 3000 HU and 31 different lung tissue types ranging from 20 to 950 HU. The remaining 5 types were chosen from subsets 2 to 6 in Table I. Also shown in Table I is the CT number range over which the materials were characterized. Pixels having CT numbers less than 20 were considered as air and were assigned a CT number of 0 in the transformation process.

V. CONCLUSIONS

A method has been developed whereby a material can be assigned to each voxel of a CT data set. The material is

derived from the Hounsfield values of the voxel. The choice of materials is such that the doses obtained by Monte Carlo calculations using these materials are not expected to differ by more than one percent from the doses which would exist in the real tissues present in the patient.

It has to be pointed out that this method has been verified for a 100 cm^2 circular field size of an 8 MV photon beam only. It is possible that for other beam energies different bin widths may have to be used to obtain the same degree of accuracy. The same may also be true for different field sizes. This is the subject of further investigation by the authors.

[a]Corresponding author: Phone: (2751) 405-2104; Fax: (2751) 4475029; Electronic mail: gnbifcp@med.uovs.ac.za

[1]W. R. Nelson, H. Hirayama, and D. W. O. Rogers, The EGS4 Code System SLAC-Report-265, Stanford Linear Accelerator Center (1985).

[2]J. A. Halbleib and T. A. Melhorn, ITS: The Integrated TIGER Series of Coupled Electron/Photon Monte Carlo Transport Codes, Sandia Report SAN84-0073, Sandia National Laboratories, Alberquerque, New Mexico.

[3]J. F. Briesmeister, Ed., MCNP-A General Monte Carlo N-Particle Transport Code, Version 4A, Los Alamos Scientific Laboratory Report LA-12625-M (1993).

[4]PEREGRINE, Lawrence Livermore National Laboratories, http://www-phys.llnl.gov/peregrine/

[5]D. W. O. Rogers and A. F. Bielajew, Monte Carlo Techniques of Electron and Photon Transport for Radiation Dosimetry, in *The Dosimetry of Ionizing Radiation*, edited by K. R. Kase, B. E. Bjärngard, and F. H. Attix (Academic, New York, 1990), Vol. III, Chap. 5.

[6]D. W. O. Rogers, B. A. Faddegon, G. X. Ding, C.-M. Ma, J. We, and T. R. Mackie, ''BEAM: A Monte Carlo code to simulate radiotherapy treatment units,'' Med. Phys. **22**, 503–524 (1995).

[7]C. Manfredotti, U. Nastasti, R. Marchisio, C. Ongaro, and G. Gervino *et al.*, ''Monte Carlo simulation of dose distribution in electron beam radiotherapy treatment planning,'' Nucl. Instrum. Methods Phys. Res. A **291**, 646–654 (1990).

[8]ICRU, International Commission On Radiation Units and Measurements, ''Tissue Substitutes in Radiation dosimetry and measurements,'' Report No. 44, Bethesda, MD, CRU, 1989.